Stem Cell Reports
Report
OPEN ACCESS

Germline Stem Cell Heterogeneity Supports Homeostasis in *Drosophila*

Amanda Yunn Ee Ng,[1,3] Kimberly Rae Guzman Peralta,[2,3] and Jun Wei Pek[1,*]
[1]Temasek Life Sciences Laboratory, National University of Singapore, 1 Research Link, Singapore 117604, Singapore
[2]Temasek Polytechnic, 21 Tampines Avenue 1, Singapore 529757, Singapore
[3]Co-first author
*Correspondence: junwei@tll.org.sg
https://doi.org/10.1016/j.stemcr.2018.05.005

SUMMARY

Adult and embryonic stem cells exhibit fluctuating gene expression; however, the biological significance of stem cell heterogeneity is not well understood. We show that, in *Drosophila*, female germline stem cells (GSCs) exhibit heterogeneous expression of a GSC differentiation-promoting factor Regena (Rga). The *Drosophila* homolog of human SON, *dsn*, is required to maintain GSC heterogeneity by suppressing sustained high levels of Rga. Reducing the expression of Rga in *dsn* mutants restores GSC heterogeneity and self-renewal. Thus, GSC heterogeneity is linked to GSC homeostasis.

INTRODUCTION

In vertebrates and invertebrates, stem cells have been shown to exhibit heterogeneous gene expression, which may be important to regulate self-renewal and differentiation into distinct lineages (Chang et al., 2008; Graf and Stadtfeld, 2008; Imayoshi et al., 2013; Kobayashi et al., 2009; MacArthur et al., 2012; Ohlstein and Spradling, 2007). *Drosophila* female germline stem cell (GSC) niche represents a simple and tractable *in vivo* model with two to three GSCs that can be identified unambiguously by their location next to the cap cells and the presence of spherical spectrosomes (Figure 1A). Although extensively used as a stem cell model, heterogeneity in gene expression has never been reported in *Drosophila* female GSCs (Lehmann, 2012; Losick et al., 2011). Here, we report that the expression of a differentiation-promoting factor Regena (Rga) is heterogeneous between GSCs in the *Drosophila* ovaries. Dsn (human homolog of SON) represses *rga* transcription and promotes GSC heterogeneity, which is important for GSC homeostasis.

RESULTS

Drosophila Female GSCs Exhibit Heterogeneous Rga Expression

Rga (NOT2 in the CCR4-NOT deadenylase complex) was reported to promote GSC differentiation, where high and low levels of Rga promote and inhibit GSC differentiation respectively (Wong et al., 2017). The expression of *rga* is being regulated by a negative feedback loop via the *sisR-1* noncoding RNA (Figure 1B) (Osman et al., 2016; Pek, 2018; Pek et al., 2015). *sisR-1* belongs to a class of stable intronic sequence RNAs that frequently regulate gene expression via feedback loops (Pek, 2018; Pek and Okamura, 2015). As previous efforts to visualize *rga* transcripts by *in situ* hybridization were unsuccessful (Wong et al., 2017), we began our study by examining the expression pattern of Rga protein in GSCs using a specific antibody against Rga (Temme et al., 2004; Wong et al., 2017). Unlike Vasa (a germline marker) that was expressed at similar levels between adjacent GSCs, Rga expression was highly heterogeneous (Figures 1C and 1D). Within the same niche, one GSC (GSC #1) expresses a higher level of Rga compared with an adjacent GSC (GSC #2), while the expression of Vasa was similar (Figures 1C and 1D). We characterized the extent of heterogeneity by measuring the levels of Rga in adjacent GSCs and calculated the ratio (see Experimental Procedures). GSCs ranged from homogeneous (ratio of 1) to highly heterogeneous (ratio of ~4.5) (Figure 1E). A ratio of 1.5 was sufficient to be scored as heterogeneous under visual inspection. Using this criterion, we observed that the expression of Rga was heterogeneous between adjacent GSCs in ~65% of the germaria examined (Figure 1F).

Heterogeneity appears to be specific to Rga as the expression of another component of the deadenylase complex CCR4 did not exhibit heterogeneity between GSCs (Figure S1A). To further investigate if heterogeneity correlates with the cell cycle, we examined the different stages of cell division using fusome morphology as a marker (Figure 1G) (de Cuevas and Spradling, 1998). Consistent with our earlier analysis, ~40% of the germaria exhibited homogeneous Rga expression (Figure S1B). Approximately 30% of the GSCs were at G1/S phase, while the remaining ~70% were at G2 phase, which is similar to what were reported in previous studies (Figure S1C) (Hsu et al., 2008; Morris and Spradling, 2011). Interestingly, when we examined the GSCs that were heterogeneous (either high or low Rga), most (>70%) of them were at G2 phase (Figure 1H); however, this was not the case for GSCs expressing homogeneous levels of Rga (Figure 1H). Furthermore, neighboring GSCs both at G2 were more heterogeneous, while

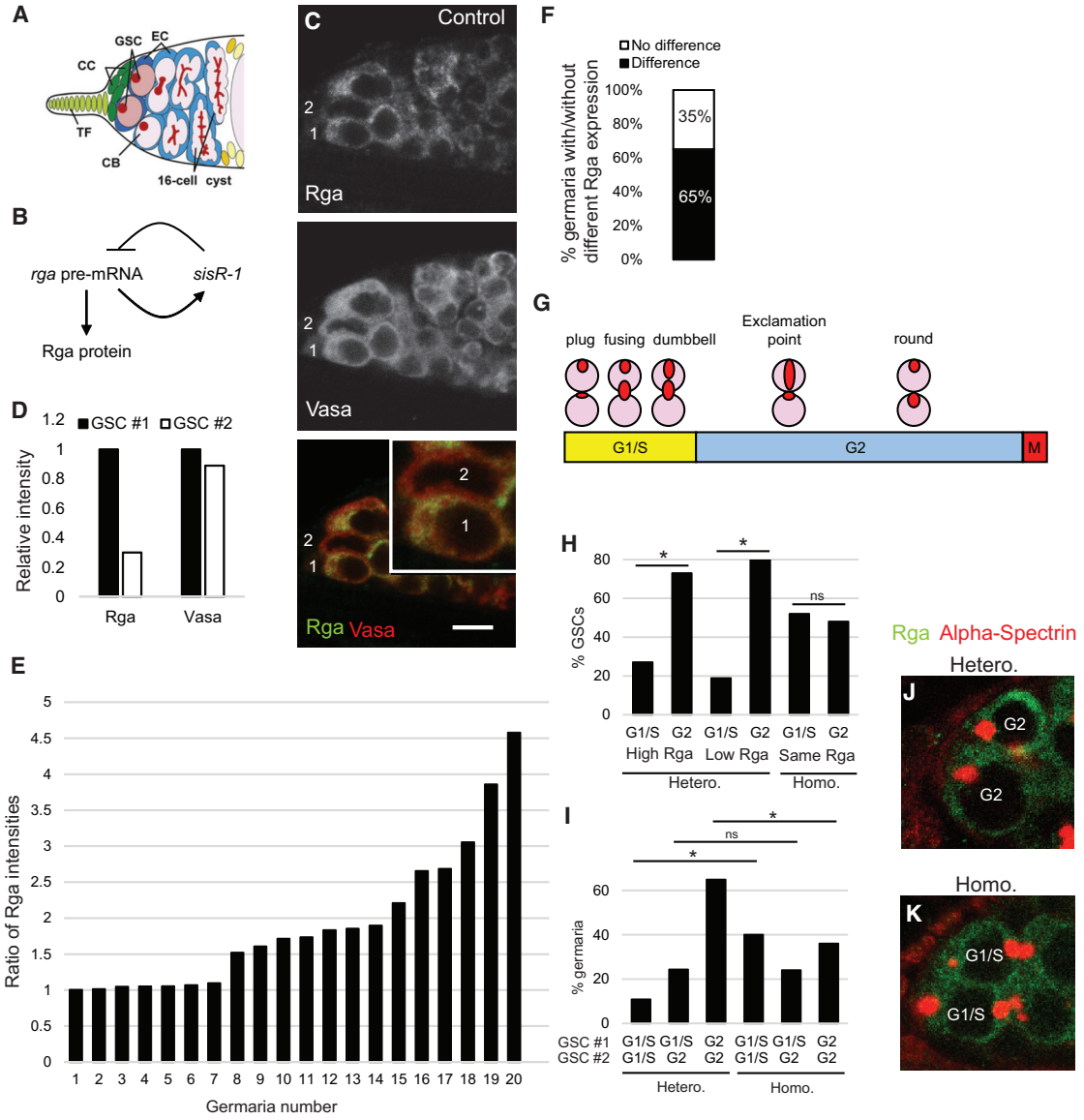

Figure 1. *Drosophila* Female GSCs Exhibit Heterogeneous Rga Expression

(A) Drawing of a germarium showing the different cell types. TF, terminal filament; CC, cap cells; GSC, germline stem cell; CB, cytoblast; EC, escort cell.

(B) The *rga-sisR-1* feedback loop. Transcription of *rga* pre-mRNA produces both *sisR-1* (from the intron) and *rga* mRNA that is translated into Rga protein. *sisR-1* represses *rga* transcription.

(C) Confocal images of a wild-type germarium stained for Rga (green) and Vasa (red). GSC #1 expresses higher level of Rga than GSC #2. Inset: magnification of GSCs #1 and #2. Scale bar: 10 μm.

(D) Chart showing the relative intensities of Rga and Vasa in GSCs #1 and #2 in (C).

(E) Chart showing the ratio of Rga intensities between GSCs in individual germaria.

(F) Chart showing the percentage of germaria with and without heterogeneous expression of Rga as depicted in (E) where cutoff was set at 1.5. n = 20 germaria.

(G) Diagram showing the scoring of cell cycle stages (G1/S and G2) according to fusome morphology.

(H) Chart showing percentages of GSCs with high, low, or homogeneous levels of Rga at G1/S or G2 stages. N = 37–50. *$p < 0.05$, two-tailed Z test. ns, $p > 0.05$.

(legend continued on next page)

those at G1/S were homogeneous (Figures 1I–1K and S1D). Therefore, our data suggest that the heterogeneity of Rga correlates with the cell cycle, with GSCs in G2 being the most heterogeneous.

dsn Represses *rga* Expression and Maintains Rga Heterogeneity in GSCs

In a screen for nuclear double-stranded RNA binding proteins that regulate *sisR-1*, we previously identified *CG8273* as a candidate gene (Wong et al., 2017). *CG8273* (called *dSon* or *dsn* hereafter) is highly expressed in the ovaries (Figure S2). *dsn* is the homolog of human SON, which is involved in transcriptional repression and splicing (Kim et al., 2016a; Lu et al., 2014; Sun et al., 2001). SON had been shown to regulate self-renewal in human embryonic stem cells and mutations in SON are associated with abnormal brain development and leukemia (Kim et al., 2016a, 2016b; Lu et al., 2013; Tokita et al., 2016).

To examine the function of *dsn*, we used a strain containing a transposon insertion at the 5′UTR of *dsn*, which dramatically reduced the expression of *dsn* mRNA (Figures 2A and 2B). In *dsn* homozygous mutant ovaries, the steady-state level of *sisR-1* was upregulated (Figure 2C). Since SON had been shown to be a transcriptional repressor and splicing enhancer, we asked if *dsn* regulates *rga* pre-mRNA (*sisR-1* precursor) expression and/or splicing. Consistent with a role in repressing *rga* transcription, *rga* pre-mRNA levels were also upregulated ~2.5-fold in *dsn* mutant ovaries compared with controls (Figure 2D). In *dsn* mutant ovaries, splicing of *rga* pre-mRNA was normal, as shown by RT-PCR using primers flanking the intron, and the levels of *rga* mRNA also increased in a similar magnitude of ~3-fold as *rga* pre-mRNA (Figures 2E and 2F). Taken together, we conclude that *dsn* primarily represses the transcription of *rga* pre-mRNA.

While we observed an increase in *rga* mRNA levels in *dsn* mutant ovaries, we did not detect an obvious change in Rga protein expression by western blotting (Figure 2G), suggesting additional feedback mechanism(s) that regulate Rga translation and/or protein stability during late oogenesis. Nevertheless, at the cellular level, we observed that, in ~85% of *dsn* mutant ovarioles, GSCs exhibited sustained high levels of Rga expression leading to a loss of heterogeneity in Rga staining (Figures 2H–2K). Adjacent GSCs (#1 and #2) now expressed similar levels of Rga, a pattern similar to that of Vasa (Figures 2H–2J). This led to a drop in the percentage of germaria with GSCs having heterogeneous Rga expression from ~65% in controls to ~15% in *dsn* mutants (Figure 2K, p = 0.00124, two-tail Z test). We conclude that *dsn* is required to maintain GSC heterogeneity by repressing the expression of *rga* pre-mRNA (Figure 2L). We suggest that, in *dsn* mutants, *rga* is upregulated leading to a higher level and perdurance of Rga protein in the GSCs, and hence loss of heterogeneity.

dsn Maintains GSC Heterogeneity and Self-Renewal by Repressing *rga*

The tuning of Rga had been previously found to regulate GSC self-renewal (Wong et al., 2017; Yan et al., 2014). Overexpression of Rga in GSCs promotes differentiation, while knockdown of Rga promotes self-renewal (Wong et al., 2017). Since Rga was upregulated in *dsn* mutant GSCs, we examined if *dsn* mutants displayed any GSC maintenance defects. We found that day 2 *dsn* mutant females laid significantly fewer eggs compared with controls (Figure 3A; control, ~53 ± 11 eggs/female/day versus *dsn* mutant, ~36 ± 5 eggs/female/day; p = 0.0003, two-tailed t test). However, the eggs hatched with similar rates as controls (Figure S3A), consistent with an unperturbed expression of Rga protein in the whole ovaries assayed by western blotting (Figure 2G). At day 21, the egg laying phenotype became more severe (Figure 3A; control, ~60 ± 14 eggs/female/day versus *dsn* mutant, ~20 ± 4 eggs/female/day; p < 0.0001, two-tailed t test), suggesting a GSC defect. Closer examination of the GSCs revealed a significant decrease in GSC number in *dsn* mutant ovaries relative to controls (Figures 3B and 3C; control, ~2.4 ± 0.7 GSCs versus *dsn* mutant, ~1.2 ± 0.8 GSCs; p = 0.00006, two-tailed t test). The GSC phenotype worsened with age (Figures 3B and 3C), confirming a GSC maintenance defect. Analysis of *dsn/Df(3R)Exel6153* showed a similar GSC loss phenotype (Figures 3D and 3E; control, ~3.0 ± 1.0 GSCs versus *dsn/Df*, ~1.6 ± 1.5 GSCs; p = 0.04, two-tailed t test). Knockdown of *dsn* in the germline by a germline-specific driver *vasa-Gal4* also led to GSC loss (Figures 3F, 3G, and S3B; control, ~2.5 ± 0.9 GSCs versus *dsn* RNAi, ~1.7 ± 0.9 GSCs; p = 0.02, two-tailed t test), confirming a role of *dsn* in promoting GSC self-renewal cell autonomously.

To investigate if the GSC loss phenotype in *dsn* mutants was due to sustained high levels of Rga in the GSCs, we reduced the dosage of Rga by removing a copy of *rga* in the *dsn* RNAi background. In *dsn* RNAi ovaries, 12.5% of germaria had GSCs with Rga heterogeneity (Figures 4A–4D). When we reduced the dosage of Rga by 50% in

(I) Chart showing percentages of germaria with GSC pairs having heterogeneous or homogeneous levels of Rga at different combinations of cell cycle stages (G1/S-G1/S, G1/S-G2, or G2-G2). N = 25–37. *p < 0.05, two-tailed Z test. ns, p > 0.05.
(J and K) Confocal images depicting (J) two GSCs having heterogeneous Rga expression at G2, and (K) two GSCs having homogeneous Rga expression at G1/S.

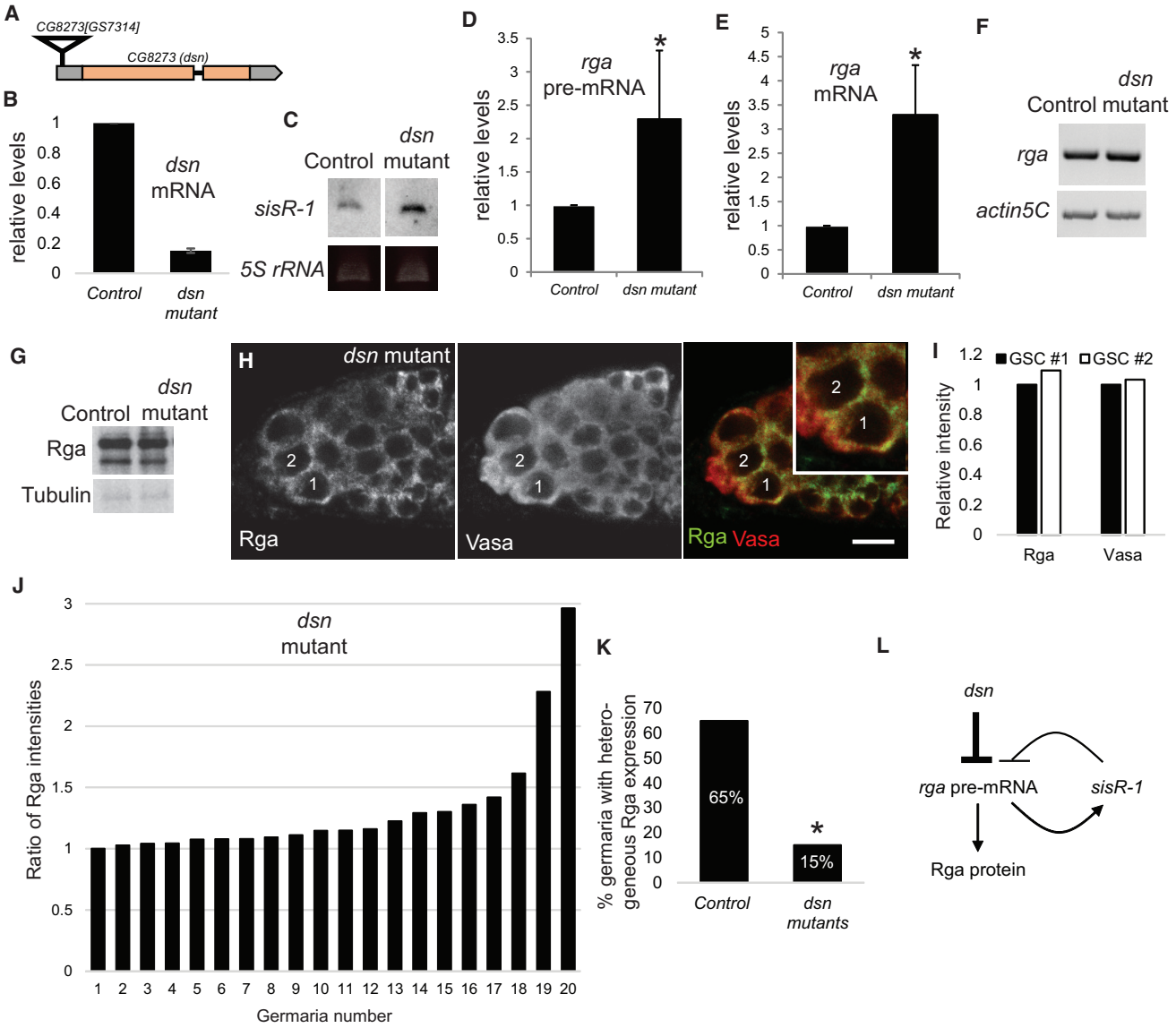

Figure 2. *dsn* Represses *rga* Expression and Maintains Rga Heterogeneity in GSCs

(A) Gene locus showing the position of the transposon insertion GS7314 in the *dsn* locus at the 5′UTR.

(B) qPCR showing the relative levels of *dsn* in *y w* control and *dsn* homozygous mutant ovaries. *Actin5C* mRNA was used as a loading control.

(C) A representative northern blot showing the abundance of *sisR-1* in control and *dsn* mutant ovaries. *5S* rRNA was used as a loading control.

(D and E) Charts showing the relative abundance of *rga* (D) pre-mRNA and (E) mRNA in control and *dsn* mutant ovaries. N = 3 biological replicates. Error bars represent SD. *p < 0.01, two-tailed t test.

(F) Gel showing RT-PCR of *rga* mRNA in control and *dsn* mutant ovaries showing correct splicing. *Actin5C* was used as a loading control.

(G) Western blot showing the abundance of Rga protein in control and *dsn* mutant ovaries. Tubulin was used as a loading control.

(H) Confocal images of a *dsn* mutant germarium stained for Rga (green) and Vasa (red). GSC #1 expresses similar level of Rga with GSC #2. Inset: magnification of GSCs #1 and #2. Scale bar: 10 μm.

(I) Chart showing the relative intensities of Rga and Vasa in GSCs #1 and #2 in (H).

(J) Chart showing the ratio of Rga intensities between GSCs in individual germaria in *dsn* mutants.

(K) Chart showing the percentages of germaria with heterogeneous expression of Rga in GSCs in control and *dsn* mutant ovaries. N = 20. *p = 0.001, two-tailed Z test.

(L) Model showing Dsn directly represses the expression of *rga* pre-mRNA independent of the *sisR-1*-mediated negative feedback loop.

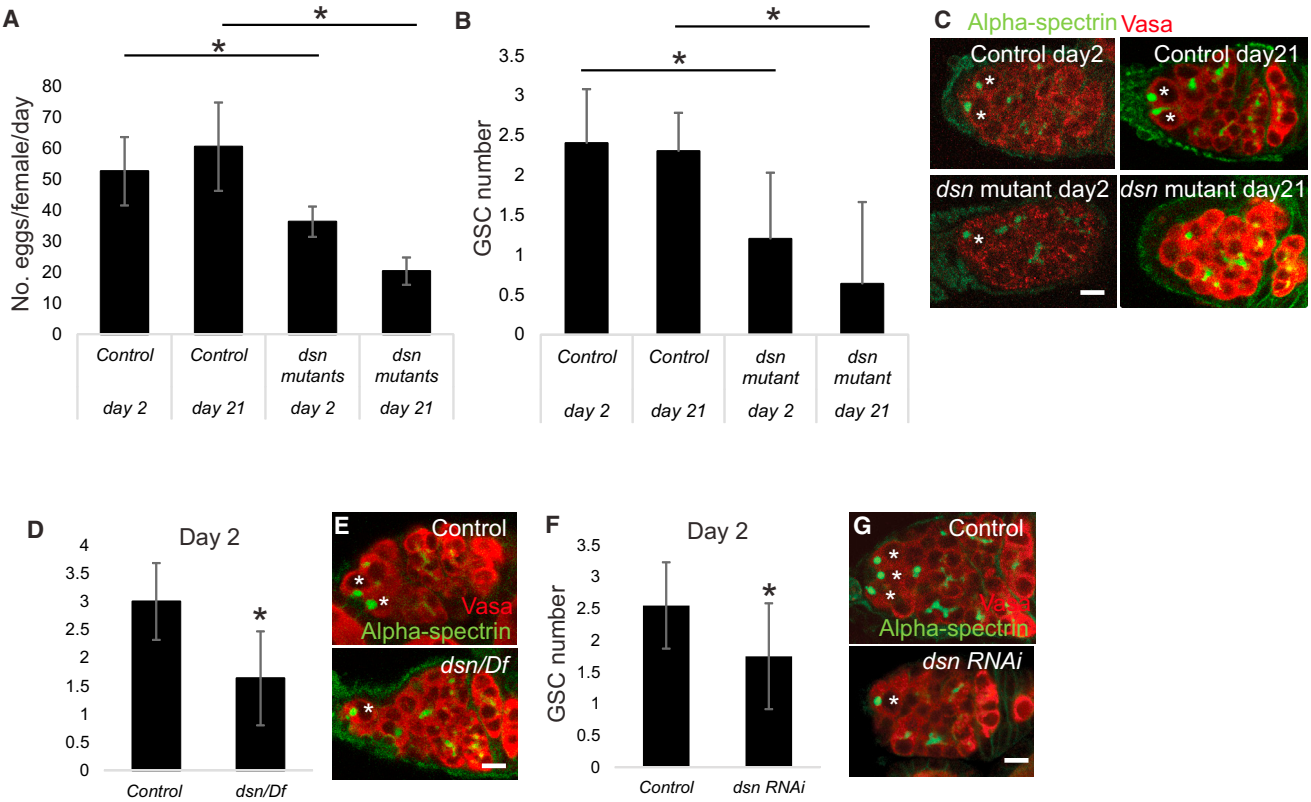

Figure 3. *dsn* Maintains GSCs

(A) Chart showing the number of eggs laid per female per day in control and *dsn* mutants at day 2 and 21 post eclosure. N = 6–10 experiments. *p < 0.001, two-tailed t test.

(B) Chart showing the number of GSCs in control and *dsn* mutant ovaries at day 2 and 21 post eclosure. N = 10–20. *p < 0.001, two-tailed t test.

(C) Confocal images showing control and *dsn* mutant germaria at day 2 and 21 post eclosure stained with alpha-spectrin (green) and Vasa (red).

(D) Chart showing the number of GSCs in control and *dsn/Df* ovaries. N = 10. *p < 0.05, two-tailed t test.

(E) Confocal images showing control and *dsn/Df* germaria stained with alpha-spectrin (green) and Vasa (red).

(F) Chart showing the number of GSCs in control and *dsn* RNAi ovaries. N = 20. *p < 0.02, two-tailed t test.

(G) Confocal images showing control and *dsn* RNAi germaria stained with alpha-spectrin (green) and Vasa (red).

*GSCs. Error bars represent standard deviation. Scale bar: 10 μm.

the *dsn* RNAi ovaries, Rga heterogeneity in GSCs reverted to normal in 56% of the germaria examined (Figures 4A–4D; *dsn* RNAi, 12.5% versus *dsn* RNAi; *rga*/+, 56%; p = 0.01, two-tail Z test). Moreover, these flies had a normal number of GSCs compared with *dsn RNAi* (Figures 4E and 4F; *dsn RNAi*, ~1.5 ± 0.9 GSCs versus *dsn* RNAi; *rga*/+, ~2.3 ± 0.9 GSCs; p = 0.01, two-tailed t test). Consistently, egg laying was also rescued back to normal (Figure 4G; control, ~70 ± 35 eggs/female/day versus *dsn* RNAi, ~28 ± 24 eggs/female/day versus *dsn* RNAi; *rga*/+, ~117 ± 47 eggs/female/day; p < 0.0001, two-tailed t test). Taken together, our genetic interaction analysis confirmed that *dsn* regulates GSC heterogeneity and self-renewal by suppressing high levels of *rga* in the GSCs.

DISCUSSION

We suggest that GSCs exhibit heterogeneous levels of Rga to coordinate self-renewal and differentiation. Prolonged overexpression of Rga triggers GSC differentiation while low Rga expression promotes GSC self-renewal (Wong et al., 2017). We envision that, at a given point of time, adjacent GSCs express different levels of Rga and are thus transiently primed toward differentiation (Figure 4H). This allows a GSC to respond rapidly and appropriately to changes in niche signals in response to changes in the environment. Since both GSCs do not respond equally, such a mechanism also creates a buffer against random fluctuations of differentiation-promoting signals that can

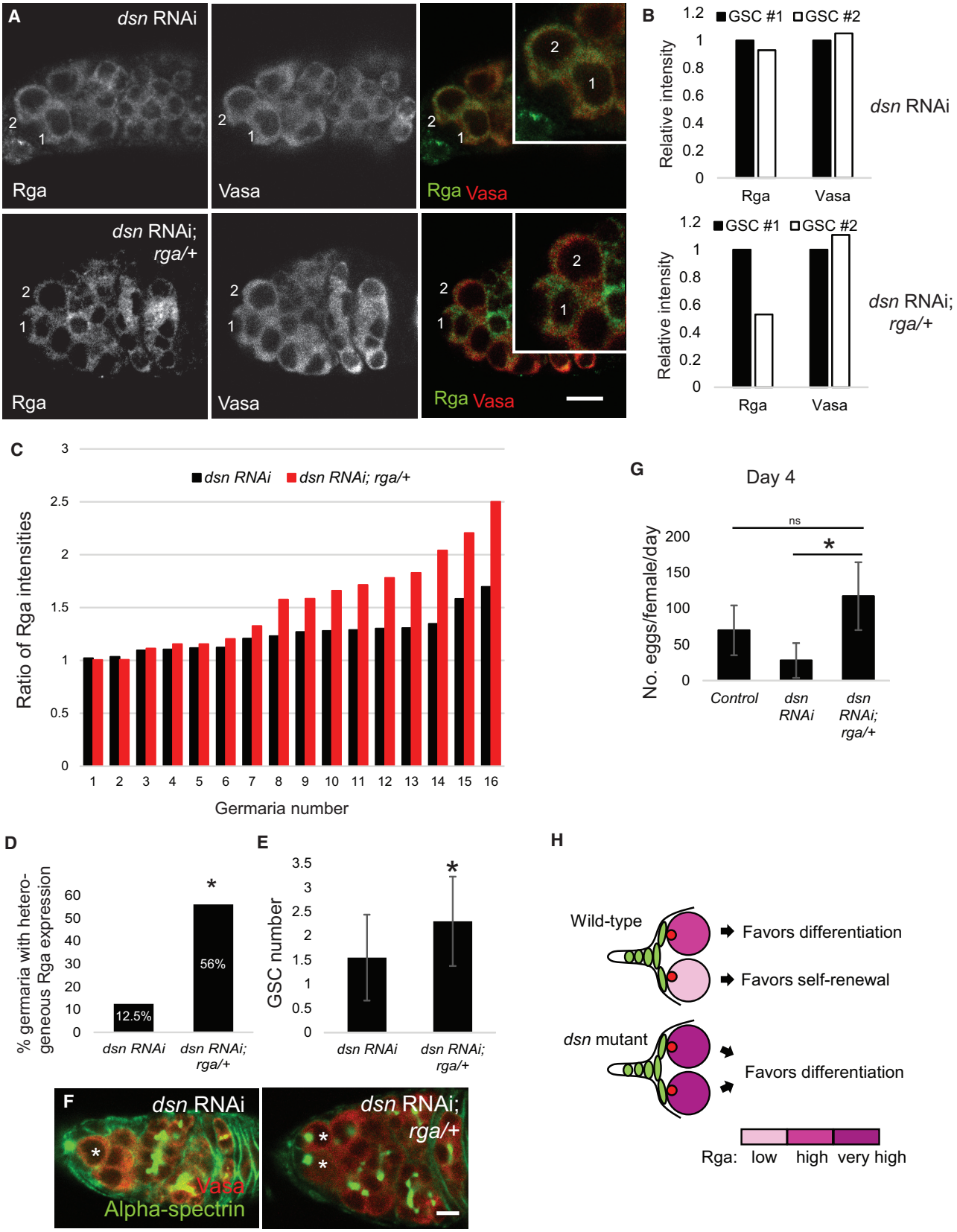

(legend on next page)

result in unwanted loss of GSCs. As G2 in GSCs is highly regulated by the insulin and TOR pathways (Hsu et al., 2008; LaFever et al., 2010), it may serve as a critical window when signaling pathways intersect with Rga to produce a graded response of self-renewal versus differentiation.

Stem cell heterogeneity has been reported and characterized in mammalian embryonic and adult stem cells such as the spermatogonial, hematopoietic, intestinal, and epithelial stem cells (Donati and Watt, 2015; Goodell et al., 2015; Graf and Stadtfeld, 2008; Krieger and Simons, 2015). Mathematical modeling had also provided support for a role of stem cell heterogeneity in balancing self-renewal and differentiation to achieve tissue homeostasis (Greulich and Simons, 2016). Our study suggests that the phenomenon of stem cell heterogeneity is also conserved in invertebrate adult stem cells. Importantly, it provides a simple model system to investigate the role of stem cell heterogeneity in tissue homeostasis.

How such Rga heterogeneity is achieved is not understood. Negative feedback loops have been proposed in other systems to generate oscillatory gene expression (Imayoshi et al., 2013; Isomura and Kageyama, 2014; Kobayashi et al., 2009; MacArthur et al., 2012). One possibility is that an oscillatory mode of Rga expression is generated by the *rga-sisR-1* negative feedback loop (Pek, 2018). The other possibilities are that Rga can fluctuate in a random manner or in response to some unknown factors during G2. In future, it would be important to understand the dynamics of Rga in GSCs. This can be achieved by long-term live imaging and quantitative analyses of the kinetics of translation and protein degradation at the single-cell level.

EXPERIMENTAL PROCEDURES

A detailed description of all methods is included in the Supplemental Information.

Fly Strains

y w flies were used a controls unless otherwise stated. The following strains were used in this study: *CG8273*^{GS7314} (Kyoto #201169), *Df(3R)6153* (Bloomington #7632), *CG8273* RNAi (TRiP HMS00114 Bloomington #34805), *MTD-Gal4* (Petrella et al., 2007), and *vasa-Gal4* (kind gift from Y. Yamashita). Flies were maintained at 25°C, while the RNAi flies at 29°C. Newly eclosed flies were fed with wet yeast paste for 2 to 21 days before dissection.

Immunostaining

Immunostaining was perform as previously described (Pek and Kai, 2011; Pek et al., 2012; Wong et al., 2017). Ovaries were fixed in a solution containing 16% paraformaldehyde and Grace's medium (2:1 ratio) for 20 min. They were then rinsed and washed in PBX (PBS containing 0.2% Triton X-100), and pre-absorbed in PBX with 5% normal goat serum. Incubation in primary antibodies was done at room temperature overnight. The next day, ovaries were washed in PBX and incubated in secondary antibodies for 4 hr at room temperature. Finally, the ovaries were washed in PBX before mounting on slides. The primary antibodies used were rabbit anti-Rga (1:500, kind gift from E. Wahle), guinea pig anti-Vasa (1:1,000, kind gift from T. Kai), mouse anti-alpha-spectrin (1:2, Developmental Studies Hybridoma Bank), and rabbit anti-CCR4 (1:500, kind gift from E. Wahle). Specificity of Rga antibody was verified previously (Wong et al., 2017). Images were taken using the Carl Zeiss LSM 5 Exciter Upright confocal microscope. Signal intensities were quantified using ImageJ software. Images were processed using Adobe Photoshop software.

Identification and Scoring of GSCs

GSCs were identified based on their location and size (Morris and Spradling, 2011) or the presence of spectrosomes. Germaria containing two GSCs clearly visible on the same confocal plane were randomly selected and Rga intensity was measured using ImageJ software. The ratios of Rga intensity of neighboring GSCs were calculated using the GSC with the lower Rga level as the denominator. Therefore, GSCs that are homogeneous will have a ratio close to 1, while those that are heterogeneous will be greater than 1. We used a cutoff of 1.5 to determine if GSCs are heterogeneous or not, because a ratio of 1.5 was sufficient to determine heterogeneity by visual inspection.

Figure 4. Loss of GSCs in *dsn* RNAi Is Due to High Levels of Rga

(A) Confocal images of *dsn* RNAi and *dsn* RNAi; *rga/+* germaria stained for Rga (green) and Vasa (red). Adjacent GSCs were labeled GSC #1 and GSC #2. Inset: magnification of GSCs #1 and #2. Scale bar: 10 μm.

(B) Chart showing the relative intensities of Rga and Vasa in GSCs #1 and #2 in (A).

(C) Chart showing the ratio of Rga intensities between GSCs in individual germaria in *dsn* RNAi and *dsn* RNAi; *rga/+* ovaries.

(D) Chart showing the percentages of germaria with heterogeneous expression of Rga in GSCs in *dsn* RNAi and *dsn* RNAi; *rga/+* ovaries. N = 16. *p = 0.009, two-tailed Z test.

(E) Chart showing the number of GSCs in *dsn* RNAi and *dsn* RNAi; *rga/+* ovaries. N = 20. *p < 0.02, two-tailed t test.

(F) Confocal images showing *dsn* RNAi and *dsn* RNAi; *rga/+* germaria stained with alpha-spectrin (green) and Vasa (red). *GSCs. Scale bar: 10 μm.

(G) Chart showing the number of eggs laid per female per day in control, *dsn* RNAi, and *dsn* RNAi; *rga/+* females. N = 6–12 experiments. *p < 0.001, two-tailed t test. ns, p > 0.05.

(H) Diagrammatic representation of how Rga heterogeneity can regulate GSC self-renewal versus differentiation.

Error bars represent standard deviation.

SUPPLEMENTAL INFORMATION

Supplemental Information includes Supplemental Experimental Procedures and three figures and can be found with this article online at https://doi.org/10.1016/j.stemcr.2018.05.005.

AUTHOR CONTRIBUTIONS

A.Y.E.N. performed northern blotting, RT-PCR, and qPCR. K.R.G.P. performed qPCR, western blotting, and fertility tests. J.W.P. performed the remaining experiments.

ACKNOWLEDGMENTS

We thank E. Wahle, T. Kai, Y. Yamashita, Developmental Studies Hybridoma Bank, Kyoto Stock Center, and the Bloomington Stock Center for reagents; and members of the Pek laboratory I. Osman and M. Tay for discussion. The authors are supported by the Temasek Life Sciences Laboratory.

Received: December 19, 2017
Revised: May 7, 2018
Accepted: May 7, 2018
Published: June 7, 2018

REFERENCES

Chang, H.H., Hemberg, M., Barahona, M., Ingber, D.E., and Huang, S. (2008). Transcriptome-wide noise controls lineage choice in mammalian progenitor cells. Nature *453*, 544–547.

de Cuevas, M., and Spradling, A.C. (1998). Morphogenesis of the *Drosophila* fusome and its implications for oocyte specification. Development *125*, 2781–2789.

Donati, G., and Watt, F.M. (2015). Stem cell heterogeneity and plasticity in epithelia. Cell Stem Cell *16*, 465–476.

Goodell, M.A., Nguyen, H., and Shroyer, N. (2015). Somatic stem cell heterogeneity: diversity in the blood, skin and intestinal stem cell compartments. Nat. Rev. Mol. Cell Biol. *16*, 299–309.

Graf, T., and Stadtfeld, M. (2008). Heterogeneity of embryonic and adult stem cells. Cell Stem Cell *3*, 480–483.

Greulich, P., and Simons, B.D. (2016). Dynamic heterogeneity as a strategy of stem cell self-renewal. Proc. Natl. Acad. Sci. USA *113*, 7509–7514.

Hsu, H.J., LaFever, L., and Drummond-Barbosa, D. (2008). Diet controls normal and tumorous germline stem cells via insulin-dependent and -independent mechanisms in *Drosophila*. Dev. Biol. *313*, 700–712.

Imayoshi, I., Isomura, A., Harima, Y., Kawaguchi, K., Kori, H., Miyachi, H., Fujiwara, T., Ishidate, F., and Kageyama, R. (2013). Oscillatory control of factors determining multipotency and fate in mouse neural progenitors. Science *342*, 1203–1208.

Isomura, A., and Kageyama, R. (2014). Ultradian oscillations and pulses: coordinating cellular responses and cell fate decisions. Development *141*, 3627–3636.

Kim, J.H., Baddoo, M.C., Park, E.Y., Stone, J.K., Park, H., Butler, T.W., Huang, G., Yan, X., Pauli-Behn, F., Myers, R.M., et al. (2016a). SON and its alternatively spliced isoforms control MLL complex-mediated H3K4me3 and transcription of leukemia-associated genes. Mol. Cell *61*, 859–873.

Kim, J.H., Shinde, D.N., Reijnders, M.R.F., Hauser, N.S., Belmonte, R.L., Wilson, G.R., Bosch, D.G.M., Bubulya, P.A., Shashi, V., Petrovski, S., et al. (2016b). De novo mutations in SON disrupt RNA splicing of genes essential for brain development and metabolism, causing an intellectual-disability syndrome. Am. J. Hum. Genet. *99*, 711–719.

Kobayashi, T., Mizuno, H., Imayoshi, I., Furusawa, C., Shirahige, K., and Kageyama, R. (2009). The cyclic gene Hes1 contributes to diverse differentiation responses of embryonic stem cells. Genes Dev. *23*, 1870–1875.

Krieger, T., and Simons, B.D. (2015). Dynamic stem cell heterogeneity. Development *142*, 1396–1406.

LaFever, L., Feoktistov, A., Hsu, H.J., and Drummond-Barbosa, D. (2010). Specific roles of target of rapamycin in the control of stem cells and their progeny in the *Drosophila* ovary. Development *137*, 2117–2126.

Lehmann, R. (2012). Germline stem cells: origin and destiny. Cell Stem Cell *10*, 729–739.

Losick, V.P., Morris, L.X., Fox, D.T., and Spradling, A. (2011). *Drosophila* stem cell niches: a decade of discovery suggests a unified view of stem cell regulation. Dev. Cell *21*, 159–171.

Lu, X., Goke, J., Sachs, F., Jacques, P.E., Liang, H., Feng, B., Bourque, G., Bubulya, P.A., and Ng, H.H. (2013). SON connects the splicing-regulatory network with pluripotency in human embryonic stem cells. Nat. Cell Biol. *15*, 1141–1152.

Lu, X., Ng, H.H., and Bubulya, P.A. (2014). The role of SON in splicing, development, and disease. Wiley Interdiscip. Rev. RNA *5*, 637–646.

MacArthur, B.D., Sevilla, A., Lenz, M., Muller, F.J., Schuldt, B.M., Schuppert, A.A., Ridden, S.J., Stumpf, P.S., Fidalgo, M., Ma'ayan, A., et al. (2012). Nanog-dependent feedback loops regulate murine embryonic stem cell heterogeneity. Nat. Cell Biol. *14*, 1139–1147.

Morris, L.X., and Spradling, A.C. (2011). Long-term live imaging provides new insight into stem cell regulation and germline-soma coordination in the *Drosophila* ovary. Development *138*, 2207–2215.

Ohlstein, B., and Spradling, A. (2007). Multipotent *Drosophila* intestinal stem cells specify daughter cell fates by differential notch signaling. Science *315*, 988–992.

Osman, I., Tay, M.L., and Pek, J.W. (2016). Stable intronic sequence RNAs (sisRNAs): a new layer of gene regulation. Cell. Mol. Life Sci. *73*, 3507–3519.

Pek, J.W. (2018). Stable intronic sequence RNAs engage in feedback loops. Trends Genet. *34*, 330–332.

Pek, J.W., and Kai, T. (2011). A role for vasa in regulating mitotic chromosome condensation in *Drosophila*. Curr. Biol. *21*, 39–44.

Pek, J.W., Ng, B.F., and Kai, T. (2012). Polo-mediated phosphorylation of Maelstrom regulates oocyte determination during oogenesis in *Drosophila*. Development *139*, 4505–4513.

Pek, J.W., and Okamura, K. (2015). Regulatory RNAs discovered in unexpected places. Wiley Interdiscip. Rev. RNA *6*, 671–686.

Pek, J.W., Osman, I., Tay, M.L., and Zheng, R.T. (2015). Stable intronic sequence RNAs have possible regulatory roles in *Drosophila melanogaster*. J. Cell Biol. *211*, 243–251.

Petrella, L.N., Smith-Leiker, T., and Cooley, L. (2007). The Ovhts polyprotein is cleaved to produce fusome and ring canal proteins required for *Drosophila* oogenesis. Development *134*, 703–712.

Sun, C.T., Lo, W.Y., Wang, I.H., Lo, Y.H., Shiou, S.R., Lai, C.K., and Ting, L.P. (2001). Transcription repression of human hepatitis B virus genes by negative regulatory element-binding protein/SON. J. Biol. Chem. *276*, 24059–24067.

Temme, C., Zaessinger, S., Meyer, S., Simonelig, M., and Wahle, E. (2004). A complex containing the CCR4 and CAF1 proteins is involved in mRNA deadenylation in *Drosophila*. EMBO J. *23*, 2862–2871.

Tokita, M.J., Braxton, A.A., Shao, Y., Lewis, A.M., Vincent, M., Kury, S., Besnard, T., Isidor, B., Latypova, X., Bezieau, S., et al. (2016). De novo truncating variants in SON cause intellectual disability, congenital malformations, and failure to thrive. Am. J. Hum. Genet. *99*, 720–727.

Wong, J.T., Akhbar, F., Ng, A.Y.E., Tay, M.L., Loi, G.J.E., and Pek, J.W. (2017). DIP1 modulates stem cell homeostasis in *Drosophila* through regulation of sisR-1. Nat. Commun. *8*, 759.

Yan, D., Neumuller, R.A., Buckner, M., Ayers, K., Li, H., Hu, Y., Yang-Zhou, D., Pan, L., Wang, X., Kelley, C., et al. (2014). A regulatory network of *Drosophila* germline stem cell self-renewal. Dev. Cell *28*, 459–473.